Hindawi
International Journal of Chemical Engineering
Volume 2019, Article ID 2474370, 7 pages
https://doi.org/10.1155/2019/2474370

Research Article

Fire-Extinguishing Efficiency of Superfine Powders under Different Injection Pressures

Guomin Zhao,[1] **Guangji Xu**,[1] **Shuang Jin**,[1] **Qingsong Zhang**,[2] **and Zhongxian Liu**[1,3]

[1]*School of Energy and Safety Engineering, Tianjin Chengjian University, Tianjin 300384, China*
[2]*Economics and Management College, Civil Aviation University of China, Tianjin 300300, China*
[3]*Tianjin Key Laboratory of Civil Structure Protection and Reinforcement, Tianjin 300384, China*

Correspondence should be addressed to Guangji Xu; 1641369386@qq.com

Received 21 January 2019; Revised 20 March 2019; Accepted 8 April 2019; Published 2 May 2019

Academic Editor: Antonio Brasiello

Ammonium phosphate fire-extinguishing agents are one of the best substitutes for halon in many powder media. Here, 11 μm median diameter ammonium phosphate ultrafine dry powder was used as a fire-extinguishing medium. The fire-extinguishing performance of ultrafine powder under different pressures was studied by analyzing fire-extinguishing time, amount of extinguishing agent, and temperature during the fire-extinguishing process. The results show that the fire-extinguishing performance of the ultrafine powder is improved with increasing injection pressure. Finally, we used FDS software for fire simulation to study the influence of injection pressure on the extinguishing agent. The results show that the extinguishing time is shortened with increasing injection pressure. From 0.2 MPa to 1.0 MPa, the extinguishing time decreases from 34 seconds to 4 seconds.

1. Introduction

After the "Montreal Protocol" regulated by UNEP in 1987, chlorine and fluorine compounds have been the focus of extreme global attention. Environmental concerns have led to the rapid phaseout of halon. Halon substitutes are an active research area. Compared with other fire-extinguishing agents, superfine powder agents have many advantages, such as short fire-suppression time, low environment toxicity, easy long-term storage, and suitability for water-deficient areas. Consequently, more and more scholars have focused on research in superfine powder chemicals including alkali metal and phosphate salts [1–6].

In recent years, many scholars have studied the preparation of ultrafine powders, the modification of ultrafine powders, the influence of particle size on the fire-extinguishing performance of ultrafine powders, and the antiexplosion performance of ultrafine dry powder extinguishers. Zhang et al. [7] obtained a spherical, hollow ultrafine $NH_4H_2PO_4$ fire-extinguishing agent by centrifugal and airflow spray drying methods. Zhu et al. [8, 9] used a direct freezing method and a spray freezing method to obtain ultrafine $NH_4H_2PO_4$ powder with uniform particle size distribution. Ultrafine particles are favored at low concentrations, low load solutions, and fast freezing rates. Huang et al. [10] prepared 300–500 nm ultrafine $NH_4H_2PO_4$ fire-extinguishing agent via a solvent-nonsolvent method. Jun used surface modification of methyl hydrogenated silicone oil. The final product has strong anticaking property, good hydrophobicity, and a fire-extinguishing agent injection rate of 98.7%. Moore [11] and Tedeschi and Leach [12] studied the efficiency of some powders and discovered that the fire-suppression efficiency of powders obviously increased with decreasing particle size. The British company KIDD [13] produces a 0.1 μm–0.5 μm bicarbonate powder via the spray drying method. Zhang et al. [14] studied the explosion suppression efficiency of $NH_4H_2PO_4$ dry powder extinguishing agent, and the results showed that $NH_4H_2PO_4$ ultrafine extinguishing agent could inhibit the spread of deflagration flame, play an effective role in flame suppression, and slow down the propagation rate of flame; thus, it can prevent the conversion from deflagration to detonation.

In recent years, many scholars have focused on the preparation of ultrafine powder, the influence of particle size

on the fire-extinguishing performance of ultrafine powder, and the fire-extinguishing performance of composite ultrafine powder. However, only a few scholars have studied the influence of injection pressure on the fire-extinguishing performance of ultrafine powder. Some scholars simply explained the impact of injection pressure on fire-extinguishing performance in the paper but did not conduct detailed research and analysis. Here, the influence of injection pressure on the fire-extinguishing performance of ultrafine powder was studied experimentally under different injection pressure conditions. In addition, FDS software was used to simulate different injection pressure conditions, and the simulation results are similar to the experimental results.

2. Materials and Fire-Extinguishing Tests

2.1. Materials. The base material of the powder extinguishing agent is $NH_4H_2PO_4$ produced by Weidun Fire Extinguishing Equipment Co. Ltd. (Tianjin, China), and the size of the ultrafine powder is 11 μm. The driving gas in this experiment is industrial nitrogen and is produced by Tianjin Xinyiqiang Chemical Co. Ltd. (Tianjin, China). The fuel is absolute ethyl alcohol produced by Tianjin Jin Tian Uni-President Technology Co. Ltd. (Tianjin, China).

2.2. Fire-Extinguishing Tests. The experimental apparatus used for the fire-extinguishing test is shown in Figure 1. The experimentation was conducted in an enclosed space. The size of the stainless-steel test chamber is 1 m × 1 m × 1 m (length × width × height) with a 150 mm × 250 mm (length-× width) window in the front of the box. The oil pan is located in the center of the test chamber, and the size is 100 mm × 100 mm × 50 mm (length × width × height). The nozzle is located in the center of the upper part of the stainless-steel test chamber. The ignition source is located in the center of the bottom of the stainless-steel test chamber, and it is 10 cm from the bottom of the stainless-steel test chamber.

The thermocouple was placed on the center line above the metal container with six thermocouples spaced at an interval of 10 cm. The distance between the first thermocouple and the fire source is 0.1 m and that between the other thermocouples and the fire source is 0.2 m, 0.3 m, 0.4 m, 0.5 m, and 0.6 m. From the bottom to the top, the thermocouple numbers are 201, 204, 207, 210, 212, and 215. The thermoelectric couples are connected to the Agilent data acquisition instrument. The computer is connected with the Agilent data acquisition instrument to record the temperature changes throughout the test process. The change in the mass of the anhydrous ethanol was recorded by an electronic balance. The fire-extinguishing progression was studied in real-time with a digital camera.

The powder transport device mainly consists of a nitrogen bottle, powder storage tank, nozzle, powder pipe, voltage regulator, and valve. The nitrogen cylinder is the power source of the powder transport device. The pressure regulator can be adjusted to change the nitrogen output pressure according to the need so as to change the powder concentration. The powder storage tank is a 150 mm high barrel with a diameter of 100 mm. The upper part is sealed by quick flange. The nitrogen pressure is fully utilized to ensure full mixing of nitrogen and powder. The powder pipe bottom has a 45° inclined entrance to increase the powder tube capture area of the powder and prevent out powder nozzle blockage. The powder nozzle is a blind tube, and 4 round holes with diameter of 2 mm are uniformly arranged on its side wall. The nitrogen cylinder, powder storage tank, powder nozzle, pressure regulator, and valve are connected by powder-conveying hose.

We poured 200 g of ultrafine dry powder extinguishing agent into a powder storage tank. After each test, we weighed the remaining ultrafine dry powder. Next, 50 ml of anhydrous ethanol was poured into the oil pan. It was ignited, and the door was then closed. When the temperature reached 700°C, the nitrogen cylinder valve was opened to put out the fire. After the experiment, the door of the test chamber was opened and cooled to room temperature before the next test to ensure that the experiment was performed in the same air environment. The experiment was repeated three times to reduce the error.

3. Experimental Results and Discussion

The relationship between the injection pressure and the time required to extinguish the fire is shown in Figure 2. The time required to extinguish the fire decreases as the injection pressure increases. When the injection pressure is 0.1 MPa, 0.2 MPa, 0.4 MPa, 0.6 MPa, and 0.8 MPa, the corresponding extinguishing time is 35 s, 18 s, 10 s, 8 s, and 6 s, respectively. When the injection pressure changes from 0.1 MPa to 0.2 MPa, the fire-extinguishing time is shortened by about half and the slope of the straight line is the highest at this time, indicating that the fire-extinguishing performance is significantly improved from 0.1 MPa to 0.2 MPa. With increasing injection pressure, the fire-extinguishing time decreases, but the slope of the straight line gradually decreases. This indicates that the fire-extinguishing performance will not be significantly improved when the injection pressure is too high.

The relationship between the injection pressure and the dose of extinguishing agent is shown in Figure 3. The amount of extinguishing agent decreases with increasing injection pressure. When the injection pressure is 0.1 MPa, 0.2 MPa, 0.4 MPa, 0.6 MPa, and 0.8 MPa, the corresponding dose of the extinguishing agent is 108.9 g, 72.5 g, 70.5 g, 67.5 g, and 58.8 g, respectively. When the injection pressure is 0.8 MPa, the amount of the fire-extinguishing agent is 50.1 g less than that at 0.1 MPa. When the injection pressure changes from 0.1 MPa to 0.2 MPa, the slope of the straight line is the highest and the amount of the extinguishing agent is reduced by 36.4 g, indicating that the open fire performance is significantly improved. The amount of extinguishing agent decreases with increasing injection pressure, but the slope of the straight line gradually decreases. This indicates that the fire-extinguishing performance increases continuously, but not obviously, when the injection pressure exceeds 0.2 MPa.

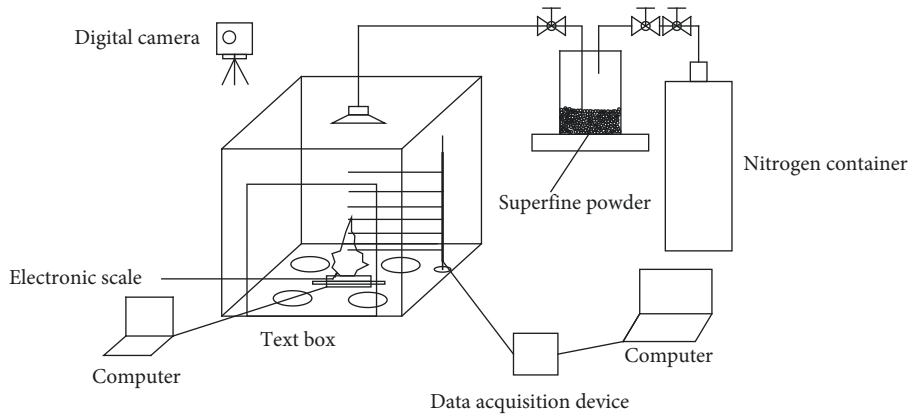

Figure 1: Schematic of the extinguishing equipment.

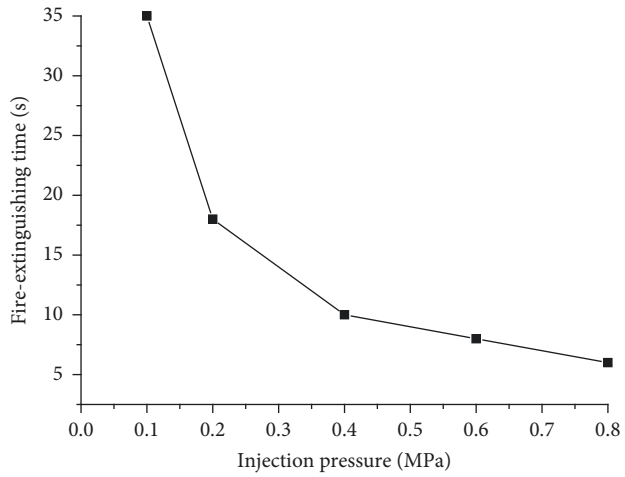

Figure 2: Fire-extinguishing time under different injection pressures.

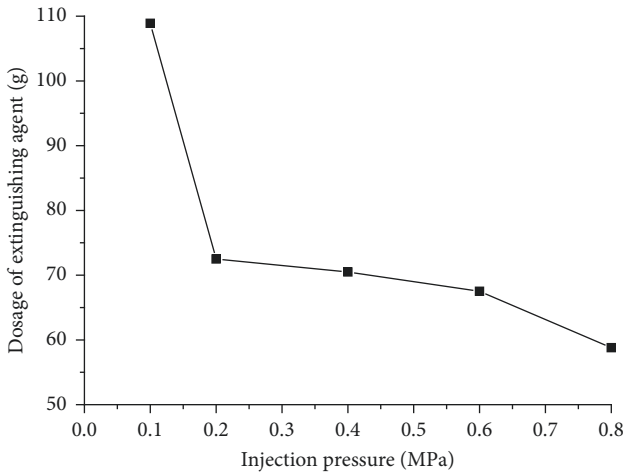

Figure 3: Dose of extinguishing agent under different injection pressures.

Figures 4(a)–4(e) show that the combustion of the test chamber temperature rises rapidly after the anhydrous ethanol is ignited, especially the nearest thermocouple (number 201) from the source of the fire. Here, the temperature rise is the fastest. The highest temperature rise is around 700°C. The rest of the thermocouples are farther from the fire source. Lower temperatures are found farther from the source. Number 204 is farther from the fire and reaches only 450°C. The sensor farthest from the fire source (#215) is only 70°C.

Figure 4(a) shows that the fire extinguishing starts at 52 s when the injection pressure is 0.1 MPa. At that point, the temperatures of thermocouples 201, 204, 207, 210, 212, and 215 are 728.566°C, 417.540°C, 278.339°C, 175.694°C, 130.475°C, and 82.500°C, respectively. After 35 s, the fire is extinguished and the corresponding temperatures are 249.981°C, 144.576°C, 106.408°C, 82.782°C, 69.322°C, and 52.39°C. The average rates of temperature drop in the fire-extinguishing process are 13.67°C/s, 7.80°C/s, 4.91°C/s, 2.65°C/s, 1.75°C/s, and 0.86°C/s.

Figure 4(b) shows that the fire extinguishing starts at 73 s when the injection pressure is 0.2 MPa. At this time, the temperatures of thermocouples 201, 204, 207, 210, 212, and 215 are 686.005°C, 470.225°C, 363.950°C, 263.149°C, 200.334°C, and 125.859°C, respectively. After 18 s, the fire is extinguished and the corresponding temperatures are 299.629°C, 203.494°C, 162.579°C, 127.841°C, 103.373°C, and 75.21°C. The average rates of temperature drop in the fire-extinguishing process are 21.47°C/s, 14.82°C/s, 11.19°C/s, 7.52°C/s, 5.39°C/s, and 2.81°C/s.

Figure 4(c) shows that the fire extinguishing starts at 53 s when the injection pressure is 0.4 MPa. At this time, the temperatures of thermocouples 201, 204, 207, 210, 212, 215 are 737.596°C, 527.646°C, 324.094°C, 187.995°C, 138.368°C, and 82.738°C, respectively. After 10 s, the fire is extinguished and the corresponding temperatures are 374.871°C, 278.114°C, 179.646°C, 128.526°C, 103.34°C, and 67.497°C. The average rates of temperature change in the fire-extinguishing process are 36.27°C/s, 24.95°C/s, 14.44°C/s, 5.95°C/s, 3.50°C/s, and 1.52°C/s.

Figure 4(d) shows that the fire extinguishing starts at 43 s when the injection pressure is 0.6 MPa. At this time, the temperatures of thermocouples 201, 204, 207, 210, 212, and 215 are 694.842°C, 420.605°C, 280.108°C, 147.554°C, 100.091°C, and 62.682°C, respectively. The fire is extinguished after 8 s, and the corresponding temperatures are 363.642°C, 252.917°C, 172.422°C, 119.861°C, 88.307°C, and

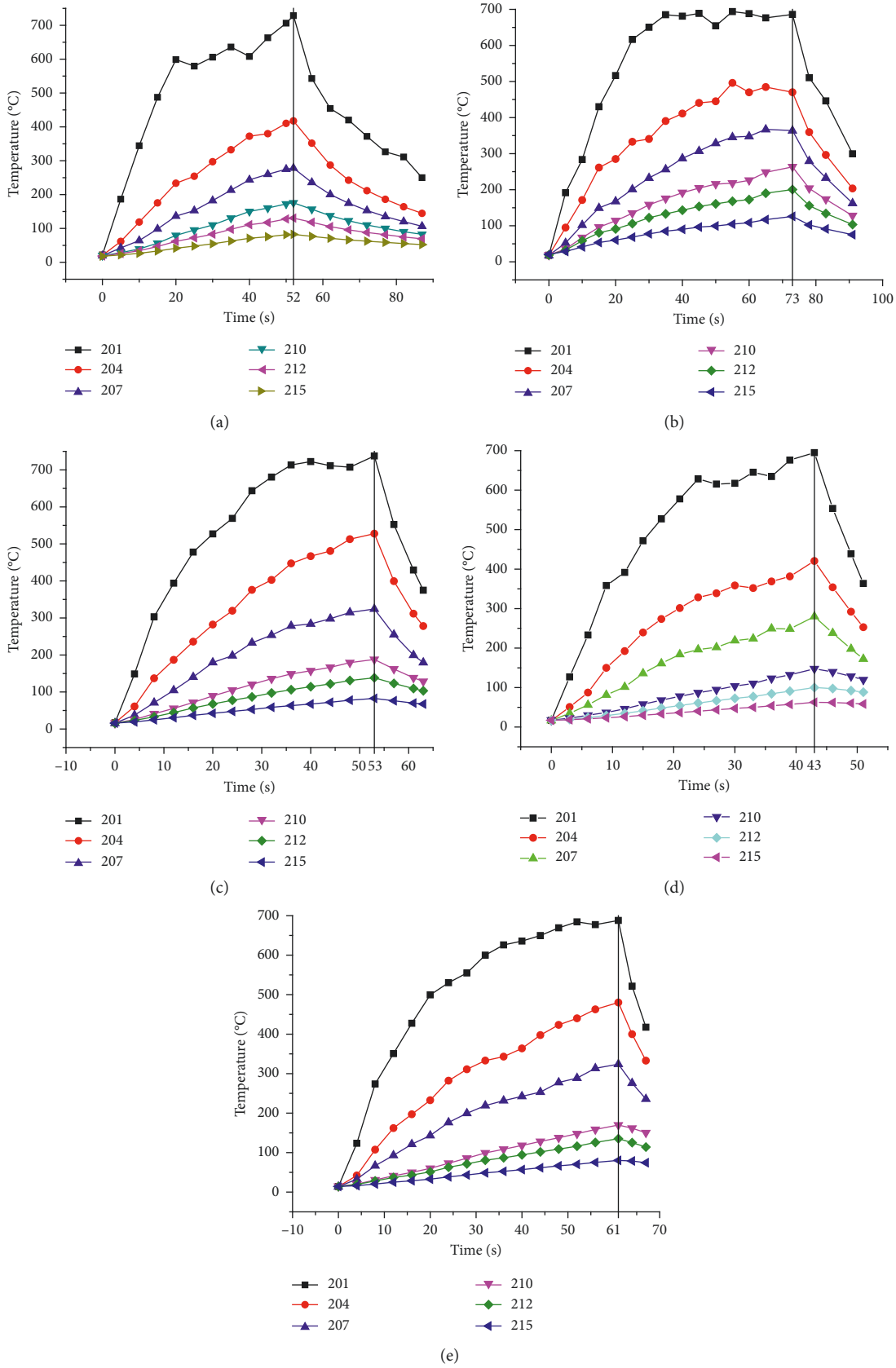

Figure 4: (a–e) Temperature field under different injection pressures. (a) 0.1 MPa. (b) 0.2 MPa. (c) 0.4 MPa. (d) 0.6 MPa. (e) 0.8 MPa.

58.537°C. This shows that the average rates of temperature drop are 41.40°C/s, 20.96°C/s, 13.46°C/s, 3.46°C/s, 1.47°C/s, and 0.52°C/s.

Figure 4(e) shows that the fire extinguishing starts at 61 s at 0.8 MPa. At this time, the temperatures of thermocouples 201, 204, 207, 210, 212, and 215 are 687.983°C, 480.215°C, 323.92°C, 169.845°C, 135.227°C, and 80.331°C, respectively. The fire is extinguished after 6 s, and the corresponding temperatures are 417.575°C, 332.921°C, 235.733°C, 150.296°C, 113.987°C, and 74.43°C. The average rates of temperature drop in the fire-extinguishing process are 45.07°C/s, 24.55°C/s, 14.70°C/s, 3.26°C/s, 3.54°C/s, and 0.98°C/s.

The average rate of temperature drop for thermocouple #201 at different injection pressures is shown in Figure 5. The rate of temperature drop increases as the injection pressure increases. The average rate of the temperature drop when the injection pressure is 0.8 MPa is about fourfold that of the average rate of temperature drop when the injection pressure is 0.1 MPa. After 0.4 MPa, the straight line tends to be flat although the average rate of temperature drop is increasing. This indicates that the cooling effect of the injection pressure on the combustion product is not very obvious. The fire-extinguishing performance is also constantly increasing as the injection pressure increases.

In summary, the fire-extinguishing performance of superfine powder increases when the injection pressure increases:

$$\begin{aligned} P &= \frac{F}{S}, \\ F - f &= ma, \\ V &= at, \\ E_k &= \frac{1}{2} mV^2. \end{aligned} \tag{1}$$

where P is the pressure on the ultrafine powder; F is the superfine powder under pressure; S is the stressed area; f is the air resistance; m is the the mass of ultrafine powder; a is the acceleration as ultrafine powder falls; V is the velocity as ultrafine powder falls; t is the time; and E_k is the kinetic energy of ultrafine powders.

When the injection pressure increases, the kinetic energy of the ultrafine powder increases before entering the plume. When the high-speed particle cloud mentioned above encounters the smoke plume formed by combustible combustion in the fire field, the ability of ultrafine powder particles as fire-extinguishing media to penetrate the smoke plume becomes stronger. This helps the extinguishing agent powder particles enter the fire field and extinguish the fire. However, if the injection pressure is too high, then the air resistance of the ultrafine powder before entering the smoke plume will also increase. This increases the kinetic energy of the ultrafine powder, but the rate of kinetic energy increase is lower. Therefore, the fire-extinguishing performance of ultrafine powder is improved when the injection pressure is too high, but this is not obvious.

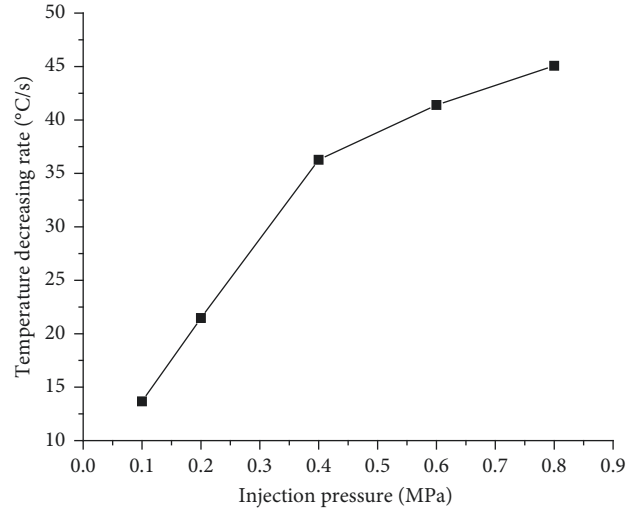

Figure 5: Rate of temperature decrease as a function of different injection pressures.

4. Simulation Experiments

4.1. About FDS Software. The FDS fire simulation software has a good computational accuracy, and the solution of fire dynamics problems can be achieved via the classical large eddy program; complex models can be created via other 3D software, and the 3D fire field problem can be solved more accurately and quickly with appropriate grid density and unique algorithm. The FDS software is a powerful tool for the study of combustion and fire dynamics. It offers a theoretical basis for solving practical problems in fire engineering. In addition, FDS has a powerful postprocessing program and data reproduction ability; FDS is an important tool in the field of fire safety research.

4.2. Fire Scenario Design. Figure 6 shows that the model grid is set to 1.2 m × 1.2 m × 1.2 m. In the simulation process, a uniform grid is adopted and the model is divided into 40 × 40 × 40 grids or 64,000 cells. Grid boundaries are set to an open form. Following the test scenario setup in the previous section, the simulation experiment is also performed in a 1 m × 1 m × 1 m box. The wall surface type of the box body is inert, and the fire source type is set to alcohol fire. The nozzle is located at the center of the upper panel of the box, and the fire is placed right below the nozzle at a distance of 80 cm. To analyze the simulation results, the temperature slices are recorded in the x direction of the test box to ensure that the temperature field in the fire-extinguishing process is directly reflected.

To simulate the effect of the injection pressure on the powder extinguishing performance in the fire-extinguishing experiment, the simulation experiment uses a spraying fire-extinguishing experiment with different injection pressures: 0.1 MPa, 0.2 MPa, 0.4 MPa, 0.6 MPa, and 0.8 MPa. In the spraying fire-extinguishing experiment, the particle type is set to solid particles and the physicochemical property of the solid particles is set according to the ammonium dihydrogen phosphate ultrafine powder extinguishing agent.

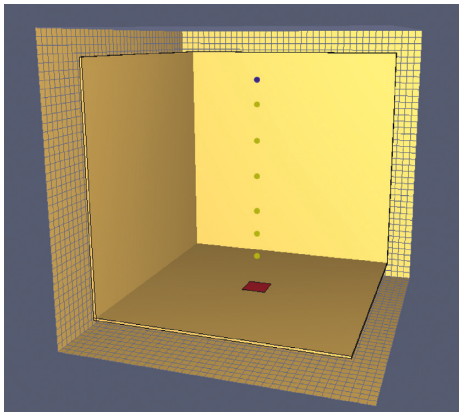

Figure 6: Fire model. The bottom square in the figure is where the fire source is placed, and 6 thermocouples are placed directly above the fire source. The distance of the thermocouple from the lower fire source is 0.25 m, 0.35 m, 0.45 m, 0.6 m, 0.75 m, and 0.9 m, respectively.

4.3. Fire Scene Settings. The simulated scenes use a spraying fire-extinguishing experiment. The sprayed particles are set as solid particles, and the solid particles are set according to the physicochemical properties of the ammonium phosphate monoammonium ultrafine powder fire-extinguishing agent. The median diameter of the solid particles is 11 μm, the spray angle is 0–60°, and the spray pressure is set as 0.1 MPa, 0.2 MPa, 0.4 MPa, 0.6 MPa, and 0.8 MPa, respectively; the spray head is set 0.95 m directly above the fire source in the spray simulation experiment. The temperature field at 0.2 MPa is simulated. The times required to extinguish the fire are simulated under different injection pressure conditions.

4.4. Results of the Simulation Experiment. An example of a temperature field in the test box in the simulation experiment is shown in Figure 7. As the figure shows, the temperature near the fire is higher throughout the entire process of the fire-extinguishing experiment (approximately 500°C). In the middle of the test box, due to the distance to the fire source, the temperature is low and varies from 100°C to 200°C. In addition, the firefighting time is approximately 17 s when the injection pressure is 0.2 MPa.

Figure 8 shows that the fire-extinguishing time decreases with increasing injection pressure. As the pressure changes from 0.1 MPa to 0.8 MPa, the firefighting time decreases from 34 s to 4 s. The fire-extinguishing time decreases with increasing injection pressure because the amount of powder injected into the fire-extinguishing box increases with increasing injection pressure. The nitrogen in the powder-storage tank then increases, and the physical and chemical fire-extinguishing effect of the extinguishing process described in Section 2.2 increases. This shortens the fire-extinguishing time. In addition, the injection pressure directly affects the release state of the powder extinguishing agent.

The fire-extinguishing time simulated by using FDS software is not much different from that in the experiment.

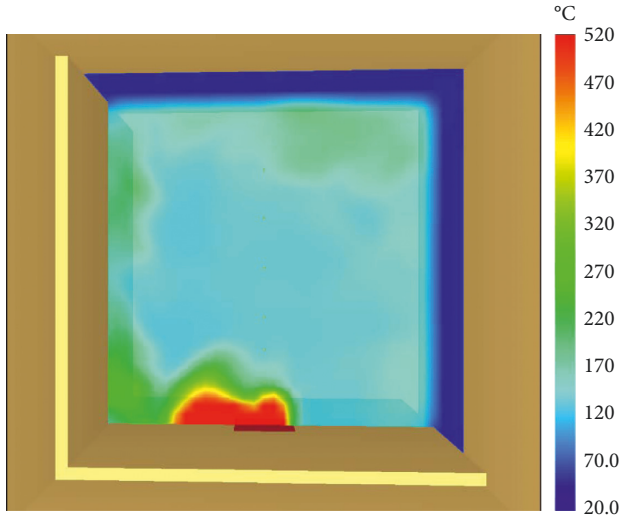

Figure 7: Temperature field in the simulation experiment.

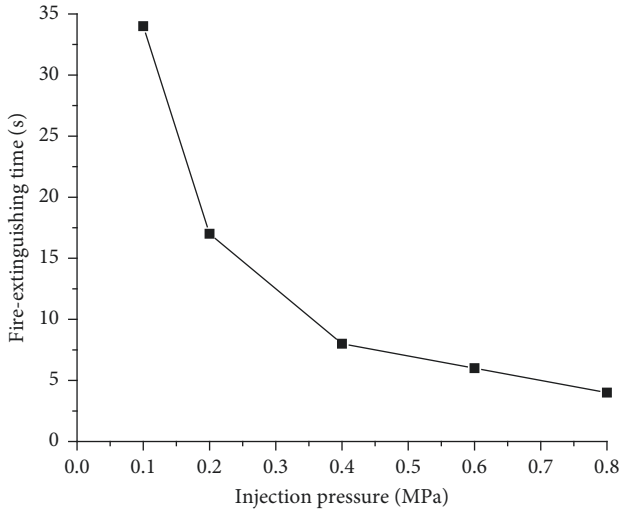

Figure 8: Variation of extinguishing time under different pressure conditions.

This might be because the simulated fire-extinguishing time is short; thus, it takes some time to open the valve door of the nitrogen cylinder to reach the injection pressure set in the experiment; thus, the fire-extinguishing time required in the experiment is relatively long. Another reason is that chemical reactions do occur during fire suppression, and FDS software does not consider this; thus, the results of the simulation and experiment will be different. However, the laws are the same.

5. Conclusions

We conclude the following:

(1) The fire-extinguishing time decreases continuously with increasing injection pressure. However, the slope of the straight line tends to be flat when the injection pressure exceeds 0.4 MPa. This increase is

not obvious when the injection pressure exceeds 0.4 MPa although the fire-extinguishing performance keeps increasing.

(2) With the increase of injection pressure, the amount of extinguishing agent is decreasing. However, when the injection pressure exceeds 0.2 MPa, the slope of the line flattens out.

(3) The average rate of temperature drop of thermocouple 201 increases with increasing injection pressure, indicating that the average rate of temperature drop increases in the temperature field near the fire source; thus, the cooling effect is good.

(4) The FDS software can be used for simulation. The fire-extinguishing time decreases with increasing injection pressure. From 0.1 MPa to 0.8 MPa, the firefighting time decreases from 34 s to 4 s.

(5) The fire-extinguishing time simulated by using FDS software is not much different from that in the experiment. One reason is that the simulated fire-extinguishing time is short, and it takes some time to open the valve door of the nitrogen cylinder to reach the injection pressure set in the experiment; thus, the fire-extinguishing time required here is relatively long. Chemical reactions also occur during fire suppression, and FDS software does not consider this. Thus, the results of the simulation and experiment will be different, but the laws are the same.

Data Availability

The data are shared to allow researchers to verify the results of the article, replicate the analysis, and conduct secondary analyses.

Conflicts of Interest

The authors declare that there are no conflicts of interest regarding the publication of this paper.

Acknowledgments

This work was supported by the National Natural Science Foundation of China (U1333123).

References

[1] Li Hong, *Experimental Study on Heat and Mass Transfer Enhancement of Falling Film Absorber in Horizontal Tube Bundle of Lithium Bromide Refrigerator*, Tianjin University, Tianjin, China, 2009.

[2] W. A. Rosser, S. H. Inami Jr., and H. Wise, "The effect of metal salts on premixed hydrocarbon-air flames," *Combustion and Flame*, vol. 7, pp. 107–119, 1963.

[3] M. Dewitte, J. Vrebosch, and A. van Tiggelen, "Inhibition and extinction of premixed flames by dust particles," *Combustion and Flame*, vol. 8, no. 4, pp. 257–266, 1964.

[4] P. Laffitte, R. Delbourgo, J. Combourieu, and J. C. Dumont, "The influence of particle diameter on the specificity of fine powders in the extinction of flames," *Combustion and Flame*, vol. 9, no. 4, pp. 357–367, 1965.

[5] J. D. Bichall, "On the mechanism of flame inhibition by alkali metal salts," *Combustion and Flame*, vol. 14, no. 1, pp. 85–95, 1970.

[6] M. Krasnyansky, "Remote extinguishing of large fires with powder aerosols," *Fire and Materials*, vol. 30, no. 5, pp. 371–382, 2006.

[7] X. Zhang, Z. Shen, and X. Fu, "Preparation and application of superfine spherical hollow ammonium phosphate fire extinguishing powder," *China Powder Technology*, vol. 16, no. 4, pp. 39-40, 2001.

[8] H. Zhu, *A New Process for Preparation of Superfine Ammonium Dihydrogen Phosphate*, Nanjing University of Science and Technology, Nanjing, China, 2009.

[9] H. Zhu, T. Ma, R. Pan et al., "Experimental study on the preparation of ultrafine dry powder extinguishing agent by freeze-drying method," in *Proceedings of the 2011 China Fire Protection Association Annual Meeting of Science and Technology*, Jinan, China, May 2000.

[10] X. Huang, L. Liu, and X. Zhou, "Experimental study on fire-extinguishing performance of ammonium phosphate sub-nanometer powder," *Fire Science*, vol. 20, no. 4, pp. 200–205, 2011.

[11] T. A. Moore, "Reducing hydrogen fluoride and other decomposition using powders and halocarbon," in *Proceedings of the Halon Option Technical Working Conference (HOTWC)*, pp. 405–415, National Institute of Standards and Technology, Albuquerque, NM, USA, May 2000.

[12] M. Tedeschi and W. Leach, "F/A-18E/F engine bay fire protection risk reduction test program," in *Proceedings of the Halon Option Technical Working Conference (HOTWC)*, pp. 349–356, National Institute of Standards and Technology, Albuquerque, NM, USA, May 1998.

[13] S. L. Zhen, *Powder Surface Modification*, Chemical Industry Press, Beijing, China, 2004.

[14] Y. Zhang, G. Zou, Y. Gao et al., "Effects of ABC dry powder on deflagration flame propagation," *Journal of Harbin Engineering University*, vol. 33, no. 4, pp. 449–453, 2012.